

Mechanical Yield in Amorphous Solids: A First-Order Phase Transition

Prabhat K. Jaiswal, Itamar Procaccia, Corrado Rainone, and Murari Singh

Department of Chemical Physics, The Weizmann Institute of Science, Rehovot 76100, Israel

(Received 10 January 2016; published 23 February 2016)

Amorphous solids yield at a critical value of the strain (in strain-controlled experiments); for larger strains, the average stress can no longer increase—the system displays an elastoplastic steady state. A long-standing riddle in the materials community is what the difference is between the microscopic states of the material before and after yield. Explanations in the literature are material specific, but the universality of the phenomenon begs a universal answer. We argue here that there is no fundamental difference in the states of matter before and after yield, but the yield is a bona fide first-order phase transition between a highly restricted set of possible configurations residing in a small region of phase space to a vastly rich set of configurations which include many marginally stable ones. To show this, we employ an order parameter of universal applicability, independent of the microscopic interactions, that is successful in quantifying the transition in an unambiguous manner.

DOI: 10.1103/PhysRevLett.116.085501

A ubiquitous, and in fact universal, characteristic of the mechanical properties of amorphous solids is their stress vs strain dependence [1]. Measured in countless quasistatic strain-controlled simulations (see, for example, [2–8]) and experiments (see, for example, [9–11]), it typically exhibits two distinct regions. In one region, at lower strain values, the stress σ increases on the average upon the increase of strain γ , although this increase is punctuated by plastic events. A second region, at higher values of the strain, displays a constant (on the average) stress which cannot increase even though the strain keeps increasing. Of course, this elastoplastic steady-state branch is also punctuated by plastic events. A typical such shear stress vs shear strain curve at zero temperature is shown in Fig. 1. The two regions are separated by what is referred to as the “yield.” The actual shape of the stress vs strain curve near the yield point depends on details of the system preparation. Amorphous solids prepared by a slow quench from the melt tend to display a stress peak before yielding, whereas those prepared by a fast quench join the steady state smoothly without a stress peak [12]. Of course, the steady-state branch itself is independent of the preparation protocol; memory of the initial state is lost in this regime.

The phenomenon of the mechanical yield in amorphous solids has been a subject of extensive study in recent years. Many numerical studies on the subject have been performed using athermal, quasistatic shear (AQS) protocols, wherein a glass is made by quenching a glass former down to zero temperature and then subjecting it to a quasistatic ($\dot{\gamma} \rightarrow 0$) shear protocol wherein the system is subject to small shear steps and then allowed, after each step, to find a new mechanically stable minimum of its potential energy. This kind of protocol always gives rise to the same basic kind of phenomenology as seen in Fig. 1 independently of the detailed microscopic interaction between the

constituents. This basic phenomenology has been reported in very many publications, and there is a general consensus about the fact that a *qualitative* change of some sort must take place between the “elastic” and “steady-state” parts of the stress-strain curve. As much as the qualitative picture is evident, however, a lot of difficulty arises when trying to capture this qualitative change in a quantitative manner.

Devising a way to distinguish and study two different states of matter, and the transition that connects one with the other, means identifying an *order parameter* to act as a

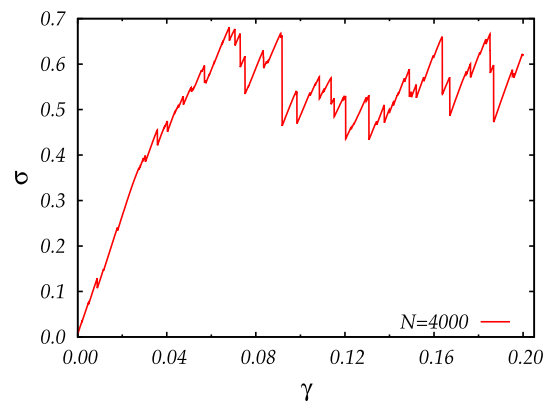


FIG. 1. A typical stress vs strain curve obtained in a strain-controlled AQS shearing protocol using a Kob-Andersen 65%–35% Lennard-Jones binary mixture of 4000 particles in 2d. Note the generic existence of a preyield branch, in which the stress is increasing on the average when the strain increases, and a postyield steady state where the average stress is constant. Both regions are punctuated by plastic events, with the stress drops being much larger in the postyield compared to the preyield branch. This kind of stress vs strain curve is ubiquitous for a huge variety of amorphous solids. Here and in the text, we drop tensorial indices from the stress and the strain for notational simplicity.

label for the states. This, however, is a challenging program in the present case: as much as the elastic and steady-state branches look different (one is able to increase the stress under a shear load, while the other cannot), a snapshot, say, of a particle configuration in both regimes is unable to detect any relevant difference between the two. Since both states are anyway amorphous, there is no trivial order parameter that would allow us to unambiguously tell them apart. Notice how this difficulty is not present in the case of crystalline solids, which *do* exhibit evident structural peculiarities with respect to liquids and whose mechanism of failure has been well known for decades. Ultimately, it all boils down to finding a suitable order parameter for the glass phase.

The problem of finding an order parameter for a glass is both practical and conceptual. First, as we said before, a snapshot of a typical glass configuration before and after yield does not show any difference: all glasses look the same to us, and all of them look like a liquid. Standard methods like structure functions, higher-order correlation functions, Voronoi tessellations, Delaunay triangulations, etc., all failed to provide distinction between typical configurations before and after yield.

In this Letter, we propose that the difficulty in making a distinction between the pre- and postyield configurations lies in the fact that *there is really no distinction*. The crux of the matter is not in the nature of configurations but in their number. The yield takes place because of a sudden opening up of a vast number of configurations that are not at the system's disposal before yield. Note that this is reminiscent of the qualitative physics predicted for the glass transition by the random-first-order-transition theory [13–15]. To establish this insight, we employ an order parameter of a type that was found useful first in the context of spin glasses [16]. Following Refs. [16–23], we can define an order parameter with the idea of comparing two different glassy configurations $\{\mathbf{r}_i^{(1)}\}_{i=1}^N$ and $\{\mathbf{r}_i^{(2)}\}_{i=1}^N$:

$$Q_{12} \equiv \frac{1}{N} \sum_i \theta(a - |\mathbf{r}_i^{(1)} - \mathbf{r}_i^{(2)}|), \quad (1)$$

wherein $\theta(x)$ is the Heaviside step function. The value of the parameter a is free and is determined by trial and error. The quantity Q_{12} is called an “overlap,” since it has a value that goes from 0 (completely decorrelated configurations) to 1 (perfect correlation). Its purpose is to measure the degree of similarity between configurations.

Let us now consider a glass, made by quenching a supercooled liquid with N particles down to a certain temperature $T \geq 0$ at a suitable rate. A glass is an amorphous solid wherein particles vibrate around an amorphous structure. So, if we take two configurations $\{\mathbf{r}_i^{(1)}\}_{i=1}^N$ and $\{\mathbf{r}_i^{(2)}\}_{i=1}^N$ from this glass, they will be most likely close to each other with Q_{12} of the order of unity. If one is able to obtain a good sampling of the typical configurations visited by the

particles in the glass, one can measure the probability distribution of the overlap $P(Q_{12})$, which will be strongly peaked around an average value $\langle Q_{12} \rangle$ close to unity. The configurations visited by the particles will then form a small connected “patch” in the configuration space of the system, selected by the amorphous structure provided by the last configuration that was visited by the liquid glass former before it fell out of equilibrium while forming a glass.

Imagine now that we begin to strain this glass. While the stress increases, there exist plastic events that begin to cause irreversible displacements in the particle positions. Our order parameter Q_{12} will begin to respond to these displacements and will begin to reduce from $O(1)$ to lower values. We will show now that all along the “elastic” branch $\langle Q_{12} \rangle$ will remain around unity, but, as the mechanical yield takes place, a sharp phase transition occurs, whereupon subextensive plastic events [24–26] begin to cause substantial displacements, allowing different regions of the configuration space to affect the order parameter. In such a situation, the distribution $P(Q_{12})$ will have two peaks: one at high $Q_{12} \leq 1$ corresponding to configurations in the same patch and one for $Q_{12} \geq 0$ corresponding to configurations in different patches.

To demonstrate this fundamental idea, we can use any model glass, since this order parameter description is expected to be universal. For concreteness we performed molecular dynamics simulations of a Kob-Andersen 65%–35% Lennard-Jones binary mixture in 2d. We have two system sizes: $N = 500$ and $N = 4000$. We chose Q_{12} with $a = 0.3$ in Lennard-Jones units but verified that changes in a leave the emerging picture invariant. As a first step, we prepared a glass by equilibrating the system at $T = 0.4$ and then quenching it (the rate is 10^{-6}) down to $T = 1 \times 10^{-6}$ into a glassy configuration. The sample is then heated up again to $T = 0.2$, and a starting configuration of particle positions is chosen at this temperature. Note that, while at $T = 0.4$ equilibration is sufficiently fast, at $T = 0.2$ the computation time is much shorter than the relaxation time. The configuration is then assigned a set of velocities randomly drawn from the Maxwell distribution at $T = 0.2$, and these different samples are then quenched down to $T = 0$ at a rate of 0.1. This procedure can be repeated any number of times (say, 500 times), and it allows us to get a sampling of the configurations inside one single patch. We verify that the typical overlap of the ensemble of inherent structures so obtained in one patch is close to $\langle Q_{12} \rangle = 1$, signaling that indeed the ensemble is completely located in a single patch. Having one patch, we repeat the procedure starting from another equilibrated configuration of the liquid to create another patch. The results shown below for the system with 4000 particles were obtained by having 100 different patches, each of which contain 500 different inherent structures due to the velocity randomization. The results with 500 particles were

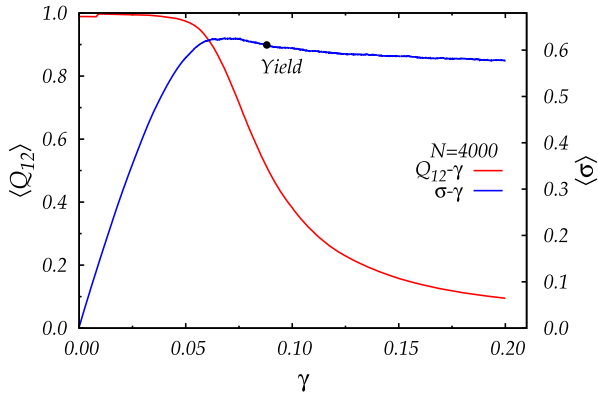


FIG. 2. A superposition of a stress vs strain curve on the dependence of $\langle Q_{12} \rangle$ on γ . The stress vs strain curve is obtained by averaging over 50 000 realizations of individual such curves obtained from 100 initial patches, each of which contain 500 inherent structures. The order parameter Q_{12} was averaged on the same realizations to provide $\langle Q_{12} \rangle$.

based on 520 different patches, each of which have 100 different inherent structures.

We then apply to each inherent structure an AQS protocol as described above. This will create for each value of γ a *strained ensemble* of configurations in the patch whose $P_\gamma(Q_{12})$ is measured. The order parameter is computed by using *all* the unique pairs of configurations generated in the strained ensemble at a given γ . We present the results for $N = 4000$ in Fig. 2. We can see how the initial ensemble for $\gamma = 0$ shows a value of the order parameter $Q_{12} = 1$, signifying that our initial ensemble is genuinely within one patch. As the ensemble is strained, the value of the order parameter gets lower, dropping towards zero when the strain is increased beyond the yield strain.

To determine the yield strain γ_Y accurately, we consider the probability distribution function (PDF) $P_\gamma(Q_{12})$. We determine $P_\gamma(Q_{12})$ for each patch of 500 configurations obtained as explained above and then average the result over the 100 available patches. We ask at which value of γ this averaged PDF has two equally high peaks; see Fig. 3. The resulting $\langle P_\gamma(Q_{12}) \rangle$ determines the yield point to occur at $\gamma_Y \approx 0.088$. Note that this criterion implies a sharp definition of yield which seems absent in the current literature. If accepted, it indicates that the mechanical yield occurs beyond the stress overshoot in correspondence with the mean-field results of Ref. [27].

Once we identify the phase transition point, we can demonstrate the transition itself. In Fig. 4, we display the change in $\langle P_\gamma(Q_{12}) \rangle$ in the vicinity of the critical point γ_Y as a function of γ . Within a very narrow range of γ , of the order of $\Delta\gamma \approx 0.017$, we observe a first-order-like transition from a PDF with a dominant peak at high values of Q_{12} to a dominant peak at low values of Q_{12} . We capture a very unambiguous and qualitative change in behavior as the yielding point is reached.

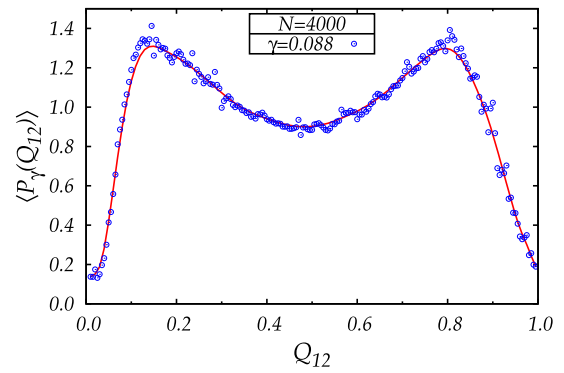


FIG. 3. The probability distribution function $P_\gamma(Q_{12})$ at $\gamma_Y = 0.088$ averaged over 100 initial configurations, each of which has 500 different realizations to obtain $\langle P_\gamma(Q_{12}) \rangle$. At this value of the strain, the PDF has two peaks of equal heights. We identify this value of γ as the point of the phase transition.

To sharpen the understanding of what is happening in the vicinity of the yield point, we examine next *how many* of our realizations lose the tight overlap with the initially prepared configuration and where the loss of overlap is taking place. To this aim we consider, for the system of 4000 particles, all the 50 000 realizations that we have. These are obtained by 100 choices of liquid realizations, each of which is velocity randomized 500 times (chosen with Boltzmann probabilities). When the strain γ is increased in our AQS algorithm, we keep computing the order parameter Q_{12} where the first configuration $\{\mathbf{r}_i^{(1)}\}_{i=1}^N$ in Eq. (1) is chosen randomly from all the available configurations at that value of γ , and the second is any one of the other available configurations at the same value of γ . We confirmed that changing the randomly chosen $\{\mathbf{r}_i^{(1)}\}_{i=1}^N$ does not affect the results. Next, choosing $Q_{12} = 0.8$ as a threshold value, we now count how many of our observed configurations cross this threshold and exhibit $Q_{12} \leq 0.8$. The number of configurations that do so as a function of the strain (superimposed on the stress vs strain curve) is shown in Fig. 5. The conclusion of this

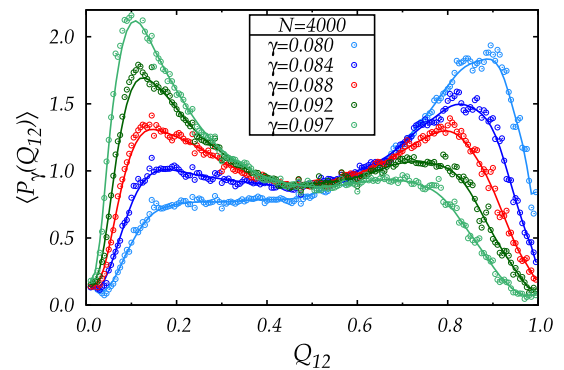


FIG. 4. The probability distribution function $\langle P_\gamma(Q_{12}) \rangle$ in the vicinity of the critical point $\gamma_Y = 0.088$.

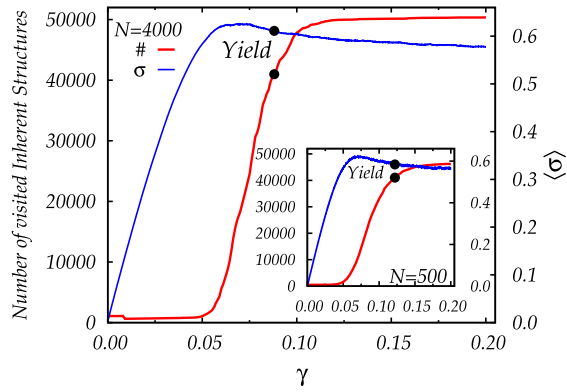


FIG. 5. The number of configurations which pass below the threshold value $Q_{12} = 0.8$ of the overlap order parameter as a function of the strain γ for $N = 4000$. In the inset, we show the same test for $N = 500$. The conclusion is that all the configurations lose overlap with the initial configuration in the vicinity of the yield point γ_Y .

test is that in the vicinity of the yield point γ_Y *all the configurations* lose their overlap with the initial configuration, but *not before*. The mechanical yield is tantamount to the opening up of a vast number of possible configurations, whereas before yield the system is still constrained to reside in the initial metabasin of the free energy landscape. This appears to be a first-order phase transition [28,29].

To strengthen the proposition that this is a first-order phase transition, we should demonstrate that the transition becomes sharper with increasing system size. At present, we cannot produce equally good data for systems of a size much larger than $N = 4000$, but we have produced equally extensive data for $N = 500$. The results for this smaller system size are presented in Fig. 6. Indeed, the change in the values of Q_{12} diminishes as seen in the upper panel, the identification of the transition point is less sharp, and, most importantly, the range of $\Delta\gamma$ over which a similar change in the peak structure is taking place is now $\Delta\gamma \approx 0.038$. If we take just these two system sizes as indicative, we can roughly estimate the range of $\Delta\gamma$ over which the transition is taking place to go to zero as $N^{-1/3}$ as $N \rightarrow \infty$. Needless to say, at this point this should be taken as indicative only, and further accurate simulations should be conducted to solidify (excuse the pun) this important issue.

The upshot of these results is that we are able to focus on the essential feature that is responsible for the mechanical yield. It is not that the configurations visited by the system after yield have different characteristics from the configurations before yield. Rather, a very constrained set of configurations available to the system before yield is replaced upon yield with a vastly larger set of available configurations. This much larger set is generic; it is not selected by any careful cooling protocol, and as such it is expected to include many marginally unstable configurations that will yield plastically with any increase of

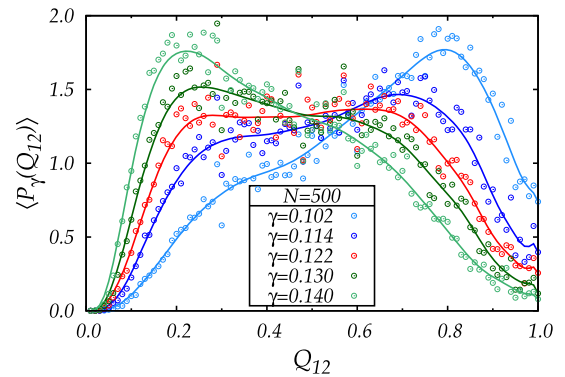
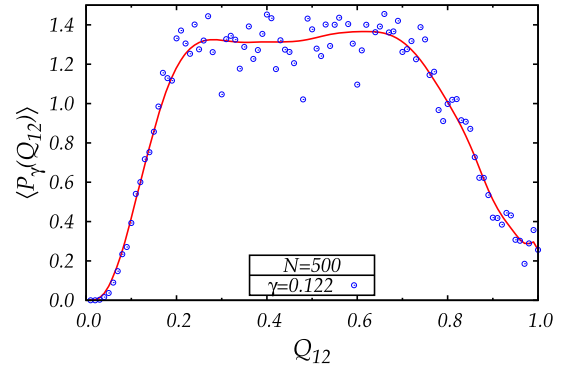
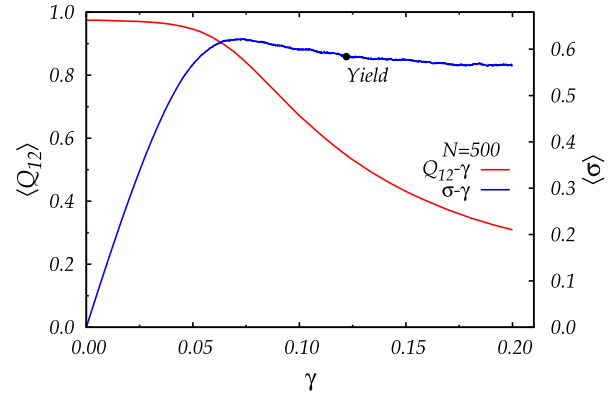


FIG. 6. Results similar to those shown in Figs. 2–4 but for system size $N = 500$. One observes a smearing out of the transition region as is expected from a first-order phase transition.

strain [30,31]. This is the fundamental reason for the inability of the system to continue to increase its stress when strain is increased, leading to the steady-state branch. We propose this as a universal mechanism for the ubiquitous prevalence of stress vs strain curves that look so similar in a huge variety of glassy systems.

This work has been supported in part by an “ideas” grant STANPAS of the European Research Council and by the Minerva Foundation, Munich, Germany. We thank Ludovic Berthier for clarifying the role of “overlap” order parameters in distinguishing amorphous configurations. Discussions with Oleg Gendelman and Carmel Shor are gratefully acknowledged.

- [1] S. Alexander, *Phys. Rep.* **296**, 65 (1998).
- [2] F. Varnik, L. Bocquet, and J.-L. Barrat, *J. Chem. Phys.* **120**, 2788 (2004).
- [3] C. E. Maloney and A. Lemaitre, *Phys. Rev. Lett.* **93**, 016001 (2004).
- [4] M. J. Demkowicz and A. S. Argon, *Phys. Rev. B* **72**, 245205 (2005).
- [5] A. Tanguy, F. Leonforte, and J.-L. Barrat, *Eur. Phys. J. E* **20**, 355 (2006).
- [6] C. E. Maloney and A. Lemaitre, *Phys. Rev. E* **74**, 016118 (2006).
- [7] E. Lerner and I. Procaccia, *Phys. Rev. E* **80**, 026128 (2009).
- [8] D. Rodney, A. Tanguy, and D. Vandembroucq, *Model. Simul. Mater. Sci. Eng.* **19**, 083001 (2011).
- [9] G. Subhash, Q. Liu, and X-L Gao, *Int. J. Impact Eng.* **32**, 1113 (2006).
- [10] A. Kara, A. Tasdemirci, and M. Guden, *Mater. Des.* **49**, 566 (2013).
- [11] A. L. Noradila, Z. Sajuri, J. Syarif, Y. Miyashita, and Y. Mutoh, *Mater. Sci. Eng.* **46**, 012031 (2013).
- [12] J. Ashwin, E. Bouchbinder, and I. Procaccia, *Phys. Rev. E* **87**, 042310 (2013).
- [13] J. P. Stoessel and P. G. Wolynes, *J. Chem. Phys.* **80**, 4502 (1984).
- [14] P. G. Wolynes, *J. Non-Cryst. Solids* **75**, 443 (1985).
- [15] A. Wisitsorasak and P. G. Wolynes, *Proc. Natl. Acad. Sci. U.S.A.* **109**, 16068 (2012).
- [16] S. Franz and G. Parisi, *Phys. Rev. Lett.* **79**, 2486 (1997).
- [17] C. Cammarota, A. Cavagna, I. Giardina, G. Gradenigo, T. S. Grigera, G. Parisi, and P. Verrocchio, *Phys. Rev. Lett.* **105**, 055703 (2010).
- [18] J. Yeo and M. A. Moore, *Phys. Rev. E* **86**, 052501 (2012).
- [19] L. Berthier, *Phys. Rev. E* **88**, 022313 (2013).
- [20] L. Berthier and D. Coslovich, *Proc. Natl. Acad. Sci. U.S.A.* **111**, 11668 (2014).
- [21] G. Biroli, C. Cammarota, G. Tarjus, and M. Tarzia, *Phys. Rev. Lett.* **112**, 175701 (2014).
- [22] L. Berthier and R. L. Jack, *Phys. Rev. Lett.* **114**, 205701 (2015).
- [23] A. Ninarello, L. Berthier, and D. Coslovich, *Mol. Phys.* **113**, 2707 (2015).
- [24] E. Lerner and I. Procaccia, *Phys. Rev. E* **79**, 066109 (2009).
- [25] R. Dasgupta, H. G. E. Hentschel, and I. Procaccia, *Phys. Rev. Lett.* **109**, 255502 (2012).
- [26] R. Dasgupta, O. Gendelman, P. Mishra, I. Procaccia, and C. A. B. Z. Shor, *Phys. Rev. E* **88**, 032401 (2013).
- [27] C. Rainone, P. Urbani, H. Yoshino, and F. Zamponi, *Phys. Rev. Lett.* **114**, 015701 (2015).
- [28] C. Rainone and P. Urbani, [arXiv:1512.00341](https://arxiv.org/abs/1512.00341).
- [29] V. Chikkadi, D. M. Miedema, M. T. Dang, B. Nienhuis, and P. Schall, *Phys. Rev. Lett.* **113**, 208301 (2014).
- [30] S. Karmakar, E. Lerner, and I. Procaccia, *Phys. Rev. E* **82**, 055103(R) (2010).
- [31] H. G. E. Hentschel, P. K. Jaiswal, I. Procaccia, and S. Sastry, *Phys. Rev. E* **92**, 062302 (2015).